Carbohydrate Polymers 89 (2012) 146–151

Contents lists available at SciVerse ScienceDirect

Carbohydrate Polymers

journal homepage: www.elsevier.com/locate/carbpol

Synthesis of nano cellulose fibers and effect on thermoplastics starch based films

N.R. Savadekar, S.T. Mhaske*

Department of Polymer and Surface Engineering, Institute of Chemical Technology, ICT, Matunga (E), Mumbai 400 019, India

ARTICLE INFO

Article history:
Received 10 January 2012
Received in revised form 21 February 2012
Accepted 22 February 2012
Available online 19 March 2012

Keywords:
Thermoplastic starch (TPS)
Nano-cellulose fibers (NCF)

ABSTRACT

Starch based films limit their application due to highly hydrophilic nature and poor mechanical properties. This problem was sought to be overcome by forming a nanocomposite of Thermoplastic starch (TPS) and Nano-Cellulose fibers (NCF). NCF was successfully synthesised from short stable cotton fibres by a chemo-mechanical process. TPS/NCF composite films were prepared by solution casting method, and their characterizations were done in terms of differential scanning calorimeter (DSC), morphology (SEM), water vapor permeability (WVTR), oxygen transmission rate (OTR), X-ray diffractograms, light transmittance and tensile properties. At very low concentration of NCF filled TPS composite film showed improvement in properties. The 0.4 wt% NCF loaded TPS films showed 46.10% improved tensile strength than by base polymer film, beyond that 0.5 wt% concentration tensile strength starts to deteriorate. WVTR and OTR results showed improved water vapor barrier property of TPS matrix. The DSC thermograms of TPS and composite films did not show any significant effect on the melting point of composite film to the base polymer TPS.

1. Introduction

Starch is a widely available, renewable, low cost, and biodegradable agro-polymer. For these reasons starch generates a great interest and it is considered as a promising alternative to synthetic polymers for packaging applications. The general procedure to process starchy materials involves the granular disruption by the combination of temperature, shear and a plasticizer, which is usually water and/or glycerol (Averous, 2004). As a packaging material, starch alone does not form films with appropriate mechanical properties unless it is first plasticized, or chemically modified. Common plasticizers for hydrophilic polymers, such as starch, are glycerol and other low molecular weight polyhydroxy compounds, polyethers, urea and water. As films or bag, starch could be employed as packaging for fruits and vegetables, snacks or dry products. In these applications, however, an efficient mechanical, oxygen and moisture protection is needed. Thermoplastic starch (TPS) alone often cannot meet all these requirements. In particular, because of the hydrophilic of the starch, the performance changes during and after processing, due to the water content changes. To overcome this drawback, many different routes have been reported. Research and development of bio-nanocomposite materials for food applications such as packaging and other food contact surfaces is expected to grow in the next decade with the advent of new polymeric materials and composites with inorganic nano-particles Nowadays, the largest parts of materials used in packaging industries are produced from fossil fuels and are practically un-degradable. For this, packaging materials for a foodstuff, like any other short-term storage packaging material, represent a serious global environmental problem. A big effort to extend the shelf life and enhance food quality while reducing packaging waste has encouraged the exploration of new bio-based packaging materials, such as edible and biodegradable films from renewable resources (Sorrentino, Gorrasi, & Vittoria, 2007). Biopolymer – clay nanocomposites are a new class of materials with potentially improved mechanical properties. These composites are prepared by addition of low amounts of clay to the biopolymer matrix (Zhao, Torley, & Halley, 2008). The main challenge for preparing nanocomposites is the nanoscale dispersion of clay in the biopolymer matrix. Montmorillonite is the most commonly used natural clay and has been successfully applied in numerous nanocomposite systems (Giannelis, 1996; Paul & Robeson, 2008; Pavlidou & Papaspyrides, 2008; Raquez, Narayan, & Dubois, 2008; Ray & Okamoto, 2003). A number of researchers have presented work in the field of starch-based bionanocomposites, which can be obtained by filling a thermoplastic starch matrix with nanofillers such as layer silicates, carbon nanotubes, carbon black, cellulose and starch nanocrystals. Montmorillonite (Huang, Yu, & Ma, 2006; Kampeerapappun, Aht-Ong, Pentrakoon, & Srikulkit, 2007) and kaolinite (Zhao, Wang, & Li, 2008) is the usual layer silicates used in starch-based bionanocomposites. Cellulose nanocrystals or whiskers have been used to reinforce starchy material (Angles & Dufresne, 2000; Angles & Dufresne, 2001; Kvien, Sugiyama, Votrubec, & Oksman, 2007;

* Corresponding author. Tel.: +91 222 33612412.
E-mail addresses: st.mhaske@ictmumbai.edu.in, st.mhaske@ictmumbai.edu.in (S.T. Mhaske).

0144-8617/$ – see front matter © 2012 Elsevier Ltd. All rights reserved.
doi:10.1016/j.carbpol.2012.02.063

Mathew & Dufresne, 2002). Cellulose is the most abundant natural polymer found in nature, and considerable interest has been recently focused on finding new material applications for this biopolymer. One of these applications has been the development of cellulose nanocrystals. It is well known that native cellulose, when subjected to strong acid hydrolysis, can be readily hydrolyzed to micro or nanocrystalline cellulose (Beck-Candanedo, Roman, & Gray, 2005; Bondeson, Mathew, & Oksman, 2006; Samir, Alloin, & Dufresne, 2005; Zhang, Elder, Pu, & Ragauskas, 2007). Cellulose whiskers and their use as a reinforcing material in composites is a relatively new field within nanotechnology that has generated considerable interest in the last decade, especially within the biopolymer community. Aqueous and solvent solution casting is the most common method of preparing cellulose nanocomposites (Dufresne, Kellerhals, & Witholt, 1999; Kvien & Oksman, 2007; Petersson, Kvien, & Oksman, 2007; Pu et al., 2007; Roman & Winter, 2002). Since 1995, publications describing the use of cellulose whiskers as reinforcing fillers (Favier, Canova, et al., 1995; Favier, Chanzy, & Cavaille, 1995; Gauthier & Perez, 1995) have resulted in an unparalleled increase in interest in producing new polymeric nanocomposites reinforced with cellulose-based nanowhiskers, nanocrystals, and nanofibers, instead of cellulose fibers (Choi & Simonsen, 2006; Favier, Canova, Shrivastava, & Cavaille, 1997; Helbert, Cavaille, & Dufresne, 1996; Roman & Winter, 2002; Samir, Alloin, Sanchez, & Dufresne, 2004; Wang, Sain, & Oksman, 2007; Wongpanit et al., 2007). Both biodegradable polymeric matrices (such as starch (Choi & Simonsen, 2006; Lu, Weng, & Cao, 2006; Mathew & Dufresne, 2002), soy protein (Lu, Weng, & Zhang, 2004), silk fibroin (Wongpanit et al., 2007), polylactide (PLA) (Huang et al., 2006), or poly(vinyl alcohol) (PVA) (Zhang et al., 2007) and nonbiodegradable polymeric matrices (such as polypropylene (Ljungberg et al., 2005), poly(vinyl chloride) (PVC) (Chazeau, Cavaille, & Perez, 2000), poly(oxyethylene) (Samir et al., 2005), or epoxy resin (Shimazaki et al., 2007) have been utilized in making nanocomposites containing cellulose nanowhiskers, nanocrystals, or nanofibers as fillers. However, in comparison with their conventional microcomposite counterparts filled by microscale cellulose fibers, these nanocomposites exhibit some outstanding properties as a result of the nanometer size effect (from only few to several hundred nanometers in width) from the nanowhiskers, nanocrystals, and nanofibers (Samir et al., 2005; de Souza Lima & Borsali, 2004). In addition, the reported large specific interfacial area (greater than 100 $m^2 g^{-1}$) (Favier, Canova, et al., 1995), high aspect ratio (up to 100) (Samir et al., 2005), high elastic modulus (up to 145 GPa (Giga Pascal)) and high Young's modulus (up to 150 GPa) (Sturcova, Davies, & Eichhorn, 2005).

The goal of this work is to study the effect of nano-cellulose fibers (NCF) concentration on the properties of TPS. TPS was used as a matrix with water and glycerol as a plasticizer and with 0.1%, 0.2%, 0.3%, 0.4%, 0.5%, and 1% NCF as reinforcements.

2. Experimental

2.1. Materials

Thermoplastic starch soluble (TPS), Extra pure procured from s.d. fine chem. Ltd., Mumbai, India. Cotton fibers (CF) were provided by CIRCOT (Mumbai, India). Acetic acid glacial (99–100%) was from Merck Specialities Private Ltd., Mumbai, India. Glycerol purified (Glycerine) eas from s.d. fine chem. Ltd., Mumbai, India.

2.2. Synthesis of nano cellulose fibers

NCF were prepared from short staple cotton by chemo-mechanical process using a lab disc refiner. Short staple cotton fibers (var: 'Bengal Desi') were soaked in the caustic solution (1% NaOH) with material to liquor ratio of 1:20. To this, 0.2 ml of nonyl phenol ethylene oxide per 100 ml was added as a wetting agent. The vessel containing cotton fibers with caustic solution was autoclaved (kier boiling) for 1 h at 15 psi to remove waxy and/or noncellulosic materials. Then this was bleached by using sodium silicate and hydrogen peroxide. For further bleaching the cotton fibers were washed with distilled water and dried in an oven at 50 °C. The cotton fibers were suspended in water and passed through the lab disc refiner and are based mainly on a narrow gape treatment of the cotton fibres to achieve the nanofibrillation. (Karande, Bharimalla, Hadge, Mhaske, & Vigneshwaran, 2011).

2.3. Preparation of TPS/NCF composite films

The preparation of TPS/NCF films was based on a solution casting and evaporation process. The varied amount of NCF (0.1%, 0.2%, 0.3%, 0.4%, 0.5%, and 1%, w/w of TPS) was dispersed into the 95 ml of distilled water under continuous stirring at 1000 rpm for 15 min. After that designated weights of TPS (5%) were mixed and stirred for the complete dissolution of TPS. Glycerol content based on TPS was fixed at 30 wt% and Acetic acid 20 wt% TPS. Glycerol and acetic acid were mixed and heated at 70 °C for 30 min with stirring until the mixture was gelatinized. The water was evaporated at room temperature overnight after that solution was poured into acrylic mould. Film formed uniformly and removed smoothly. Average film thickness formed was 0.60 mm.

3. Characterizations

3.1. Tensile properties

The tensile strength and percent elongation of films were determined using Universal Testing Machine (LR-50 K, LLOYD instrument, UK) with 500 N load cell, in accordance to ASTM D 882.

3.2. Differential scanning calorimeter (DSC)

DSC was used to measure thermal transitions of TPS films and nanocomposite films. The test was performed with Q100 DSC (TA Instruments) equipment, fitted with a nitrogen-based cooling system. The samples were weighed in aluminium pans and hermetically sealed; an empty pan was used as reference. All the measurements were performed in the range −50 to 150 °C at a heating rate of 10 °C/min.

3.3. X-ray diffractometer

X-ray Diffraction (XRD) patterns were obtained using a Rigaku Miniflex X-ray Diffractometer using Cu target and having X-ray wavelength of 1.54 Å. The sample was placed in a sample holder, and analysis is carried out in a static position, and detector moving through angle 2 to 60°.

3.4. Water vapor transmission rate (WVTR)

Water Vapor Transmission Rates (WVTR) values of the films were determined gravimetrically according to ASTM E96 method. Each test film was sealed on the top of permeation cells containing distilled water. The permeation cells were placed in desiccators maintained at 0% RH. RH 0 was maintained using anhydrous calcium chloride in a cell. The composite films were cut into circles and sealed over the cell with melted paraffin. The water transferred through the film and absorbed by the desiccant was determined from the weight of the permeation cell. Anhydrous calcium chloride ($CaCl_2$) was used as a desiccant. Each permeation cell was weighed

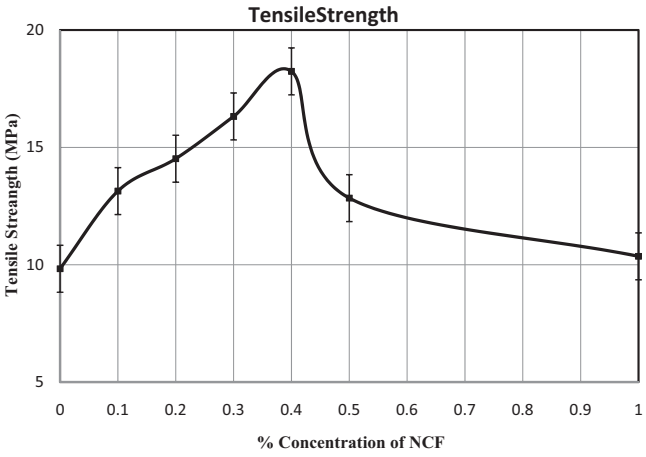

Fig. 1. Tensile strength of TPS/NCF composite film and Control TPS film.

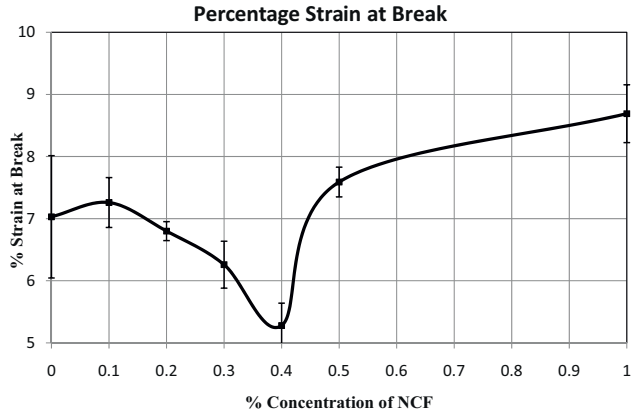

Fig. 2. Percentage strain at Break of TPS/NCF composite film and Control TPS film.

at an interval of 24 h. The WVTR was expressed in gm mm/cm^2 per day.

3.5. Oxygen transmission rate (OTR)

OTR of the films was determined using an oxygen transmission rate test machine (Labthink BTY-B1). After a film was placed in a cell and oxygen flow was introduced on 1 side of the films, and the oxygen transmission rate (OTR) was measured. OTR in (cm^3/m^2 d Pa) was calculated from the mean OTR multiplied by the film thickness (μm) and divided by the oxygen gradient in the cell of the testing machine (1 kgf/cm^2).

3.6. Light transmittance testing of the films

The light transmittance (Tr) of the PS and TPS/NCF films with a thickness of 0.60 mm was measured using an ultraviolet–visible (UV–Vis) spectroscope (UV-160A, Shimadzu, Japan) at a wavelength range of 200–800 nm.

3.7. Morphology (SEM)

The morphology of NCF was observed by a scanning electron microscope (SEM). SEM analysis was carried out with the JEOL® 6380 LA (Japan) Scanning Electron Microscope. Samples were fractured under liquid nitrogen to avoid any disturbance to the molecular structure and the specimens were coated with gold before imaging.

4. Results and discussion

4.1. Mechanical properties of the films

Figs. 1 and 2 show the tensile properties of the TPS/NCF composite films. Tensile properties such as tensile strength (TS) and elongation at break (%*E*) have been evaluated from the experimental stress–strain curves obtained for all prepared nanocomposite films. The Tensile strength and % elongation at break values of the neat TPS film were 9.83 MPa (Megapascal) and 7.03%, respectively. When comparing tensile strength of the TPS/NCF films (Fig. 1), it was obvious that addition of NCF helped to improve the tensile strength of the films. TS increased with the increasing of NCF content up to 0.4% its showed 46.10% improvement. The tensile strength value of TPS/NCF 0.5% and 1% composite film (12.84 MPa and 10.35 MPa, respectively) was lower than those of the TPS/NCF 0.4% film. This indicated that due to the heterogeneous size distribution and agglomerations of NCF within the TPS matrix, NCF did not act as reinforcing filler in TPS. On the other hand, excess of NCF content was a likely cause of phase separation, poor particle distribution and larger agglomerates formation, which led to poor mechanical properties as proven by decreased tensile strength (0.5 and 1 wt%).

The preparation of TPS/NCF composite could improve the tensile properties of the base polymer. Hence, NCF addition was found to enhance as well as impair the tensile properties depending on the level of loading. Percentage strain at break decreases with the increases percentage of NCF of the base polymer.

4.2. Differential scanning calorimeter (DSC)

The calorimetric thermograms for all samples are depicted in Fig. 3 and given as heat flow (mW) vs temperature (*T*). Due to the nature of DSC where the relative heat between the sample and the reference was measured; the relative thermal capacity is the primary result. The DSC thermograms of TPS and composite films samples showed that the transitions occur over a quite broad temperature range. Fig. 3 it does not show any significant effect on the melting point of composite film to the base polymer TPS, but addition of 0.5% NCF it slightly shifted to lower temperature.

4.3. X-ray diffractometer

The X-ray diffraction (XRD) patterns recorded for NCF and TPS nanocomposites after conditioning are shown in Fig. 4. The NCF diffractrogram displayed well-defined peaks, typical of a highly crystalline structure. The peak at $2\theta = 14.7^\circ$, $2\theta = 16.3^\circ$, $2\theta = 22.6^\circ$,

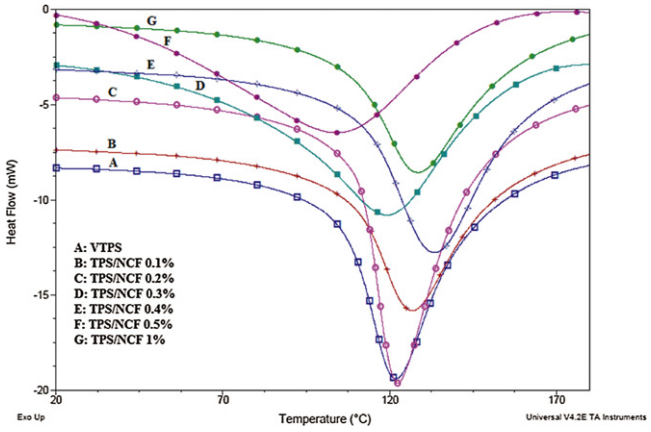

Fig. 3. DSC thermograms of TPS/NCF composite film and Control TPS film.

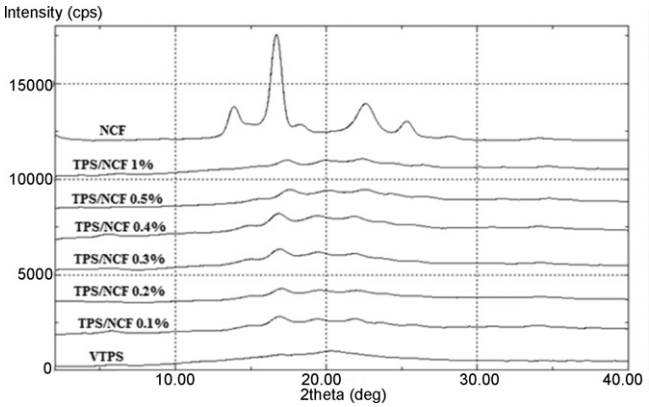

Fig. 4. XRD of TPS/NCF composite film and Control TPS film.

and $2\theta = 34.7^{\circ}$ corresponds to the (101), (10−1), (002), and (040) crystallographic planes, respectively, (Sun et al., 2007; Wang, Kumar, & Zhang, 2009) which were characteristic of cellulose type I. (Klemm, Heublein, Fink, & Bohn, 2005)

The NCF is crystalline materials therefore increase the concentration of NCF increase the crystalline regions increase the rigidity of cellulose nanowhiskers (Alemdar & Sain, 2008). As described later, the expected tensile strength of the composite materials could be enhanced by using these NCF with higher rigidity as fillers in polymer matrices. Percentage crystallinity of nanocomposite film increases with increasing the percentage of NCF with in starch matrix but up to 0.4 wt% after that its goes down.

4.4. Water vapor transmission rate (WVTR)

The specific water vapor transmission rate (WVTR) of the TPS and composite films was shown in Fig. 5. TPS is hydrophilic in nature and hence it has high WVTR. The high WVTR is decreased by the presence of dispersed phase of NCF into the TPS biopolymer matrix. But elongate of water particles path decreased this WVTR in nanocomposite film. This nanocomposite consists of dispersed phase of NCF into TPS biopolymer matrix. The NCF particles act as a barrier for water vapor which results in the drop of water vapor transmission rate through the starch biopolymer matrix/NCF composite films. WVTR of TPS/NCF composites decreased with increase the NCF content. 7.8×10^{-3} g/h/sq m. was the highest WVTR permeated easily through control TPS film. Significant decrease in WVTR value (4.3×10^{-4} g/h/sq m.) was recorded as the NCF content increased up to 0.4 wt%. Further increase in NCF content increase the WVTR value slight. However is was still lesser than that of control WVTR value of TPS. This phenomenon can be explained by

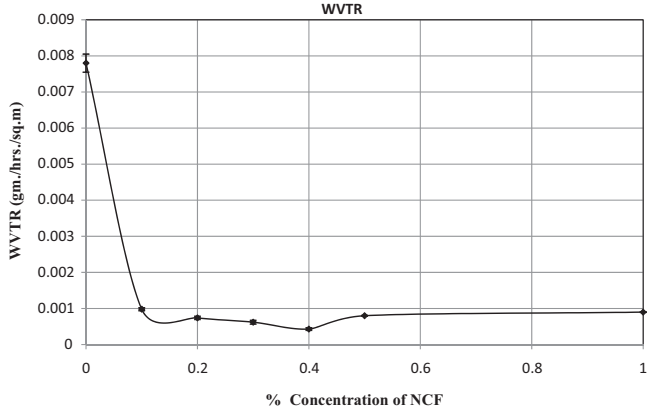

Fig. 5. WVTR of TPS/NCF composite film and Control TPS film.

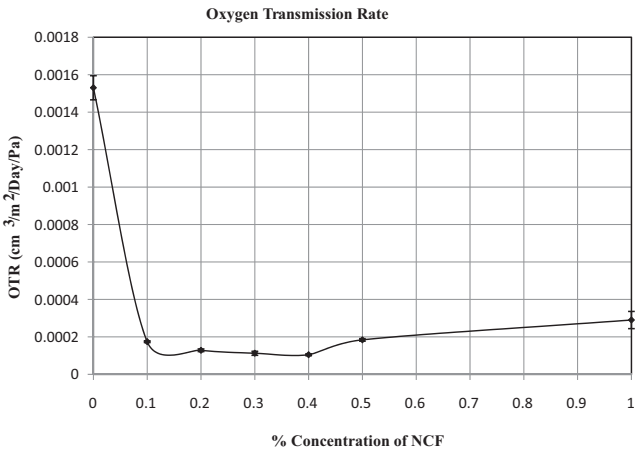

Fig. 6. OTR of TPS/NCF composite film and Control TPS film.

the addition of NCF which enables a tortuous path for the water molecules to pass through.

4.5. Oxygen transmission rate (OTR)

Fig. 6 showed the OTR versus percentage of nano cellulose fibers. From Fig. 6, it is seen that the oxygen permeability is most largely reduced, i.e. by 93%, in the 0.4% NCF/TPS compared to the control TPS sample. Starch has high oxygen permeability but the decrease in OTR of nanocomposite films due to which generates a more tortuous path for the permeation of oxygen molecules presence of NCF dispersed phase into the TPS biopolymer matrix.

4.6. Light transmittance testing of the films

The light transmittance (Tr) of the selected films in the wavelength range of 200–800 nm was shown in Fig. 7. The Tr value of TPS/NCF film was significantly lower than that of the neat TPS film at the same wavelength, indicating that the filling of NCF in TPS decreased the transparency of the films. The Tr value at 800 nm reflects the transparency of the films, which also provides some information on the particle size and degree of dispersion of the fillers within the matrix (Chen, Liu, Chang, Anderson, & Huneault, 2009). For example, at a wavelength of 800 nm, the Tr values of TPS/NCF 1 wt% and TPS were 62% and 88%, respectively. However in the case of 0.1 wt% and 0.2 wt% NCF, the Tr values were improved 92% and 94%, respectively. And for other composition Tr, value decreases with increased content of NCF as compared to control matrix TPS film. The results from the transmittance measurement of the films at wavelengths from 200 to 800 nm showed

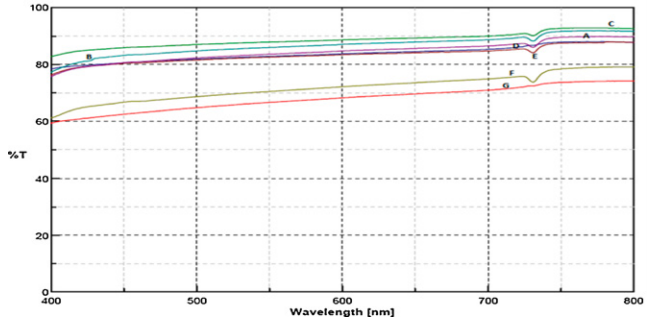

Fig. 7. Light transmittance (Tr) of A: TPS, B: TPS/NCF 0.2%, C: TPS/NCF 0.1%, D: TPS/NCF 0.3%, E: TPS/NCF 0.4%, F: TPS/NCF 0.5% and G: TPS/NCF 1% films in the wavelength range from 400 to 800 nm.

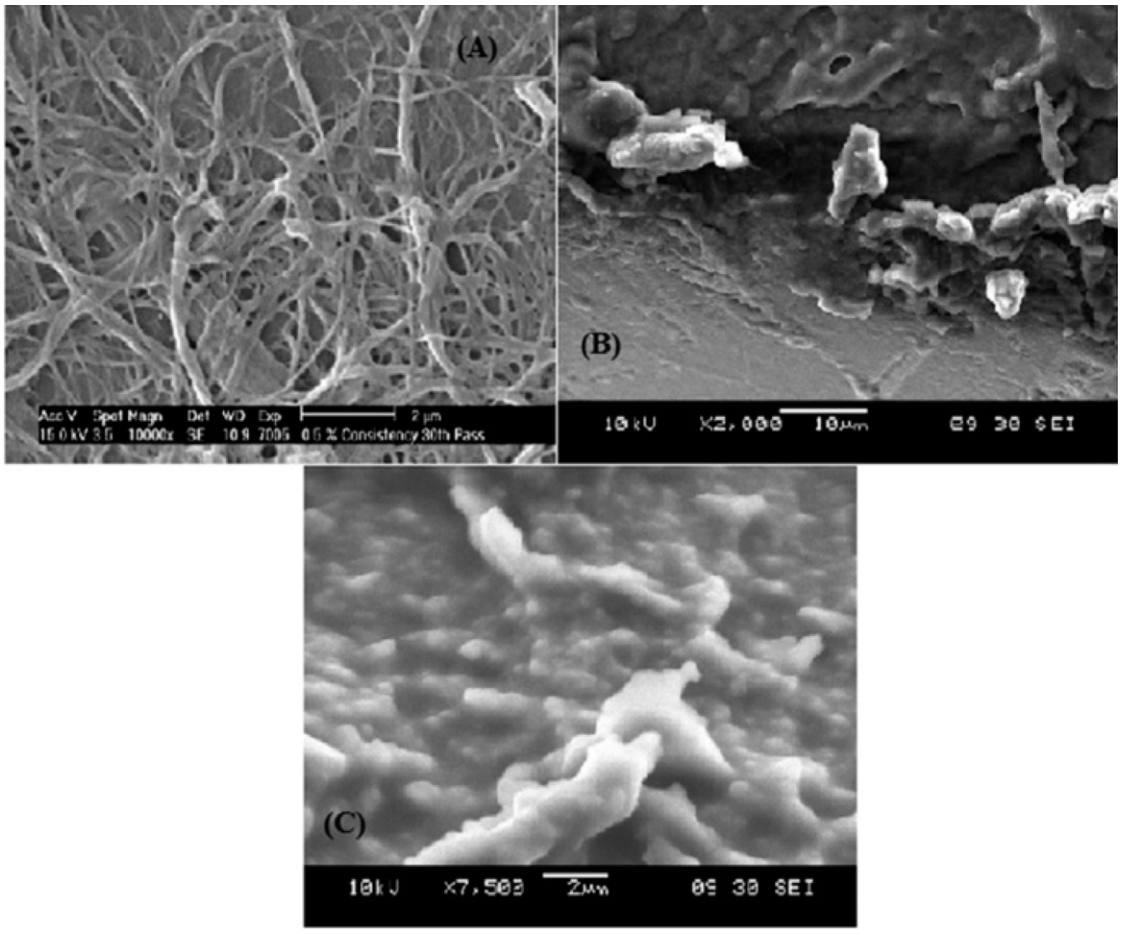

Fig. 8. SEM photograph of NCF (A), the cross sections of TPS/NCF 0.4% (B), the cross sections of TPS/NCF 1% (C).

that the addition of NCF into TPS improved the performance of anti-ultraviolet radiation while keeping or enhancing the transparency of the resulting nanocomposite films.

4.7. Morphology (SEM)

From Fig. 8(A) SEM analysis, it was observed that the diameter of the fibril 242 ± 158 nm. Fig. 8(B and C) was the SEM micrographs of the samples which were fractured under liquid nitrogen, 0.4 wt% NCF filled TPS and 1 wt% NCF filled TPS, respectively. For each material, different magnifications were used in order to display both the cellulose dispersion within the TPS matrix and the interfacial adhesion between the composite components. The incorporation of NCF substrates had a modest effect on the TPS, since no residual TPS granular structures were observed after the composite processing. The SEM micrographs Fig. 8(B) (TPS/NCF 0.4 wt%) also provide the evidence of the strong interfacial adhesion between the NCF and the TPS matrix. The strong interfacial adhesion is a result of their good dispersion within the matrix. Tensile strength improves to 46.10%, due to good dispersion and no noticeable agglomerate of NCF. Obviously, in the case of 1 wt% NCF filled TPS (Fig. 8C), poor interfacial adhesion between the NCF, and the TPS matrix observed. This poor interfacial adhesion is the result of agglomeration of NCF which has subsequently reduced its tensile strength. The uneven structure and agglomeration of the 1 wt% NCF filled TPS can be the cause of higher water vapor transmission rate.

5. Conclusions

NCF was successfully extracted from short stable cotton fibres by a chemo-mechanical process. This study provides an initial insight into the use and characteristics of NCF in TPS based biocomposites film. While compared with the control TPS film and the TPS/NCF film, nanocomposite films showed higher tensile strength; reduced percentage elongation at break; decreased water vapor rate transmission and oxygen transmission rate. This is due to the factors such as the nanometer size effects of the NCF (high L/D), the high content of cellulose crystalline regions, the homogeneous dispersion of NCF within TPS, and the strong interaction between NCF and TPS matrix. The SEM result indicates, agglomerate formation in higher concentration (i.e. 1 wt% Fig. 8C) because of nanometer length size effect.

Acknowledgements

The authors are thankful to National Agricultural Innovation Project (NAIP), Indian Council of Agricultural Research (ICAR) for the kind support through its Sub-project entitled ‘Synthesis and characterization of CNW and its application in biodegradable

polymer composites to enhance their performance', code number "C2041".

References

Alemdar, A., & Sain, M. (2008). Isolation and characterization of nanofibers from agricultural residues – Wheat straw and soy hulls. *Bioresource Technology*, *99*(6), 1664–1671.

Angles, M. N., & Dufresne, A. (2000). Plasticized starch/tunicin whiskers nanocomposites 1. Structural analysis. *Macromolecules*, *33*(22), 8344–8353.

Angles, M. N., & Dufresne, A. (2001). Plasticized starch/tunicin whiskers nanocomposite materials 2. Mechanical behavior. *Macromolecules*, *34*(9), 2921–2931.

Averous, L. (2004). Biodegradable multiphase systems based on plasticized starch: A review. *Journal of Macromolecular Science Part C Polymer Reviews*, *C44*(3), 231–274.

Beck-Candanedo, S., Roman, M., & Gray, D. G. (2005). Effect of reaction conditions on the properties and behavior of wood cellulose nanocrystal suspensions. *Biomacromolecules*, *6*(2), 1048–1054.

Bondeson, D., Mathew, A., & Oksman, K. (2006). Optimization of the isolation of nanocrystals from microcrystalline cellulose by acid hydrolysis. *Cellulose*, *13*(2), 171–180.

Chazeau, L., Cavaille, J. Y., & Perez, J. (2000). Plasticized PVC reinforced with cellulose whiskers II. Plastic behavior. *Journal of Polymer Science: Part B: Polymer Physics*, *38*(3), 383–392.

Chen, Y., Liu, C., Chang, P. R., Anderson, D. P., & Huneault, M. A. (2009). Pea starch-based composite films with pea hull fibers and pea hull fiber-derived nanowhiskers. *Polymer Engineering and Science*, *49*(2), 369–378.

Choi, Y., & Simonsen, J. (2006). Cellulose nanocrystal-filled carboxymethyl cellulose nanocomposites. *Journal of Nanoscience and Nanotechnology*, *6*(3), 633–639.

Dufresne, A., Kellerhals, M. B., & Witholt, B. (1999). Transcrystallization in Mcl-PHAs/cellulose whiskers composites. *Macromolecules*, *32*(22), 7396–7401.

Favier, V., Canova, G. R., Cavaille, J. Y., Chanzy, H., Dufresne, A., & Gauthier, C. (1995). Nanocomposite materials from latex and cellulose whiskers. *Polymers for Advanced Technologies*, *6*(5), 351–355.

Favier, V., Chanzy, H., & Cavaille, J. Y. (1995). Polymer nanocomposites reinforced by cellulose whiskers. *Macromolecules*, *28*(18), 6365–6367.

Favier, V., Canova, G. R., Shrivastava, S. C., & Cavaille, J. Y. (1997). Mechanical percolation in cellulose whisker nanocomposites. *Polymer Engineering and Science*, *37*(10), 1732–1739.

Gauthier, C., & Perez, J. (1995). Morphology and thermomechanical properties of latex films. *Polymers for Advanced Technologies*, *6*(5), 276–284.

Giannelis, E. P. (1996). Polymer-layered silicate nanocomposites. *Advanced Material*, *8*(1), 29–35.

Helbert, W., Cavaille, J. Y., & Dufresne, A. (1996). Thermoplastic nanocomposites filled with wheat straw cellulose whiskers Part I: Processing and mechanical behavior. *Polymer Composites*, *17*(4), 604–611.

Huang, M. F., Yu, J. G., & Ma, X. F. (2006). High mechanical performance MMT-urea and formamide-plasticized thermoplastic cornstarch biodegradable nanocomposites. *Carbohydrate Polymers*, *63*(3), 393–399.

Kampeerapappun, P., Aht-Ong, D., Pentrakoon, D., & Srikulkit, K. (2007). A re-examination and partial characterisation of polysaccharides released by mild acid hydrolysis from the chlorite-treated leaves of *Sphagnum papillosum*. *Carbohydrate Polymers*, *67*(2), 155–163.

Karande, V. S., Bharimalla, A. K., Hadge, G. B., Mhaske, S. T., & Vigneshwaran, N. (2011). Nanofibrillation of cotton fibers by disc refiner and its characterization. *Fibers and Polymers*, *12*(3), 399–404.

Klemm, D., Heublein, B., Fink, H. P., & Bohn, A. (2005). Cellulose fascinating biopolymer and sustainable raw material. *Angewandte Chemie International Edition*, *44*(22), 3358–3393.

Kvien, I., & Oksman, K. (2007). Orientation of cellulose nanowhiskers in polyvinyl alcohol. *Applied Physics A: Materials Science and Processing*, *87*(4), 641–643.

Kvien, I., Sugiyama, J., Votrubec, M., & Oksman, K. (2007). Characterization of starch based nanocomposites. *Journal of Materials Science*, *42*(19), 8163–8171.

Ljungberg, N., Bonini, C., Bortolussi, F., Boisson, C., Heux, L., & Cavaille, J. Y. (2005). New nanocomposite materials reinforced with cellulose whiskers in atactic polypropylene: Effect of surface and dispersion characteristics. *Biomacromolecules*, *6*(5), 2732–2739.

Lu, Y., Weng, L., & Cao, X. (2006). Morphological, thermal and mechanical properties of ramie crystallites—Reinforced plasticized starch biocomposites. *Carbohydrate Polymers*, *63*(2), 198–204.

Lu, Y., Weng, L., & Zhang, L. (2004). Morphology and properties of soy protein isolate thermoplastics reinforced with chitin whiskers. *Biomacromolecules*, *5*(3), 1046–1051.

Mathew, A. P., & Dufresne, A. (2002). Morphological investigation of nanocomposites from sorbitol plasticized starch and tunicin whiskers. *Biomacromolecules*, *3*(3), 609–617.

de Souza Lima, M. M., & Borsali, R. (2004). Rod like cellulose microcrystals: Structure, properties, and applications. *Macromolecular Rapid Communications*, *25*(7), 771–787.

Samir, M. A. S. A., Alloin, F., & Dufresne, A. (2005). Review of recent research into cellulosic whiskers, their properties and their application in nanocomposite field. *Biomacromolecules*, *6*(2), 612–626.

Samir, M. A. S. A., Alloin, F., Sanchez, J. Y., & Dufresne, A. (2004). Cellulose nanocrystals reinforced poly(oxyethylene). *Polymer*, *45*(12), 4149–4157.

Pavlidou, S., & Papaspyrides, C. D. (2008). A review on polymer-layered silicate nanocomposites. *Progress in Polymer Science*, *33*(12), 1119–1198.

Paul, D. R., & Robeson, L. M. (2008). Polymer nanotechnology: Nanocomposites. *Polymer*, *49*(15), 3187–3204.

Petersson, L., Kvien, I., & Oksman, K. (2007). Structure and thermal properties of poly(lactic acid)/cellulose whiskers nanocomposite materials. *Composites Science and Technology*, *67*(11–12), 2535–2544.

Pu, Y., Zhang, J., Elder, T., Deng, Y., Gatenholm, P., & Ragauskas, A. J. (2007). Investigation into nanocellulosics versus acacia reinforced acrylic films. *Composites Part B: Engineering*, *38*(3), 360–366.

Raquez, J. M., Narayan, R., & Dubois, P. (2008). Recent advances in reactive extrusion processing of biodegradable polymer-based compositions. *Macromolecular Materials and Engineering*, *293*(6), 447–470.

Ray, S. S., & Okamoto, M. (2003). Polymer/layered silicate nanocomposites: a review from preparation to processing. *Progress in Polymer Science*, *28*(11), 1539–1641.

Roman, M., & Winter, W. T. (2002). Nanocomposites of cellulose acetate butyrate reinforced with cellulose nanocrystals. *Journal of Polymers and the Environment*, *10*(1–2), 27–30.

Shimazaki, Y., Miyazaki, Y., Takezawa, Y., Nogi, M., Abe, K., Ifuku, S., & Yano, H. (2007). Excellent thermal conductivity of transparent cellulose nanofiber/epoxy resin nanocomposites. *Biomacromolecules*, *8*(9), 2976–2978.

Sturcova, A., Davies, G. R., & Eichhorn, S. J. (2005). Elastic modulus and stress-transfer properties of tunicate cellulose whiskers. *Biomacromolecules*, *6*(2), 1055–1061.

Sorrentino, A., Gorrasi, G., & Vittoria, V. (2007). Potential perspectives of bionanocomposites for food packaging applications. *Trends in Food Science & Technology*, *18*(2), 84–95.

Sun, Y., Lin, L., Pang, C., Deng, H., Peng, H., Li, J., He, B., & Liu, S. (2007). Hydrolysis of cotton fiber cellulose in formic acid. *Energy & Fuels*, *21*(4), 2386–2389.

Wang, B., Sain, M., & Oksman, K. (2007). Study of structural morphology of hemp fiber from the micro to the nanoscale. *Applied Composite Materials*, *14*(2), 89–103.

Wang, L., Kumar, R., & Zhang, L. (2009). Investigation into hemp fiber- and whisker-reinforced soy protein composites. *Frontiers of Chemistry in China*, *4*(3), 313–320.

Wongpanit, P., Sanchavanakit, N., Pavasant, P., Bunaprasert, T., Tabata, Y., & Rujiravanit, R. (2007). Preparation and characterization of chitin whisker-reinforced silk fibroin nanocomposite sponges. *European Polymer Journal*, *43*(10), 4123–4135.

Zhang, J., Elder, T. J., Pu, Y., & Ragauskas, A. J. (2007). Facile synthesis of spherical cellulose nanoparticles. *Carbohydrate Polymers*, *69*(3), 607–611.

Zhao, R., Torley, P., & Halley, P. J. (2008). Emerging biodegradable materials: starch- and protein-based bio-nanocomposites. *Journal of Materials Science*, *43*(9), 3058–3071.

Zhao, X. P., Wang, B. X., & Li, J. (2008). Synthesis and electrorheological activity of a modified kaolinite/carboxymethyl starch hybrid nanocomposite. *Journal of Applied Polymer Science*, *108*(5), 2833–2839.